Single-Parameter Prediction of Stable Crack Growth in Large-Scale Panels

V.P.Naumenko

Department of Fracture, Institute for Problems of Strength, Kyiv, Ukraine

ABSTRACT: *Predictive capabilities of the so-called Unified Methodology (UM) are examined by the use of a Transferring Law (TL), to say, a common function of the test data on moving center cracks of different length in rather small specimens made from a ductile material. A combined analysis of these data and closely corresponding evidence from the literature indicate that the TL may be used, to a first approximation, as a simple quantitative tool to predict residual strength of proportionally scaled plates at least under uniaxial tension. The various effects of in-plane constraint, among them load biaxiality, are covered by the UM analysis.*

INTRODUCTION

The mode of loading in thin-wall structures tends to be uniaxial or biaxial tension. It is highly improbable to predict stable crack growth which develops unconstrained flow fields using the R-curve concept in isolation from analyses of the global deformation pattern and necking [1, 2]. Nowadays it is generally agreed that the constant level ψ_{ss} of the Crack-Tip Opening Angle is a more fundamental fracture criterion value than K_R or J_R resistance curves. However, experimentally measured and analytically derived ψ_{ss} angles can differ significantly. From [3] it follows that for the large center-cracked panels respective values of ψ_{ss} were 5.5 and 3.4 degrees. Such type of inconsistencies between computational and experimental data demonstrates convincingly that [4]: “a universal fracture law governing slow crack growth has not been found yet”.

This paper is presented from the viewpoint of “moving crack tip” embedded into the fully-developed “moving neck”. They both spread straight across the ligament under quasistatic loading. The aim is to check the potential of the UM [2,5] against predicting an upper limit to the critical load that a large-scale panel is able to sustain under uniaxial tension.

TEORETICAL BACKGROUND IN BRIEF TERMS

A center crack in an unconstraint Problem Domain (PD) of uniform thickness B is modeled by an elliptic hole (Figure 1) having length $2c>>B$. In a stress-free PD, the hole has the fixed radii $\rho_n = b^2/c$ and $\rho_m = c^2/b$ of an extreme curvature at the points "n" and "m" on ideal crack profiles of different length. The procedure used for determination of ρ_n and ρ_m values, treated as characteristics of an actual crack in a given material, is outlined in [6]. An imaginary state of the stress-free plate relates to a virgin material, that is, to the zeroth level of a structural damage. Other important test events are the state "u" of the completely unloaded PD and the state "s" when both crack-tips are advancing under steady-state conditions.

Geometry-independent resistance to ductile tearing is only recovered under restrictive conditions of self-similar crack growth [2,5]. In an attempt to develop a simple TL, a new notion of the Steady-State Tearing (SST) has been incorporated in the analysis. The SST means that: (i) a crack is driven forward under a constant level σ_{Ns} of the net-section stress σ_N resulting from proportional increments in applied loads or displacements, and, (ii)

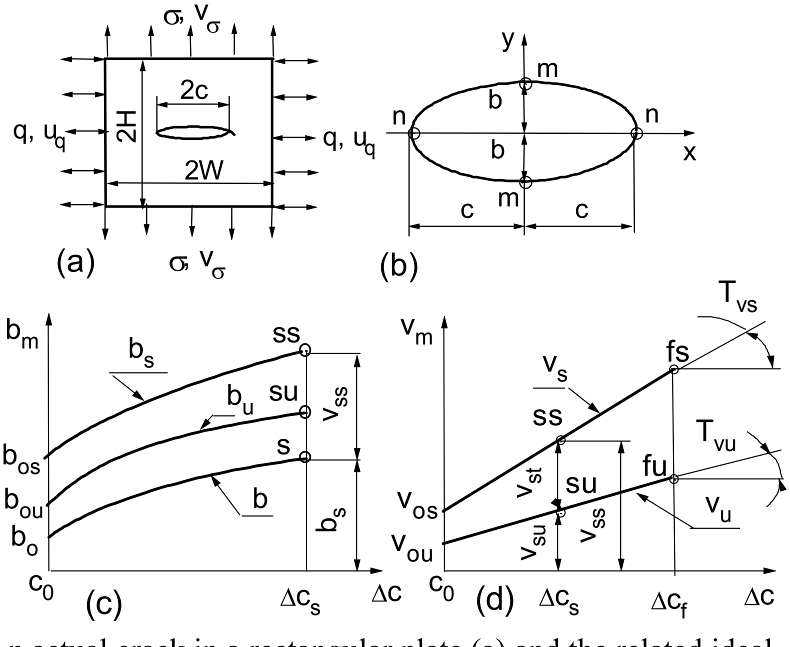

Figure 1: An actual crack in a rectangular plate (a) and the related ideal crack (b) together with postulated dependencies of the half-spacing b_m (c) and displacement v_m (d) upon the increase in the half-spacing $c_n=c$.

during omnidirectional extension of crack borders the reversible, $2v_{st}$, and irreversible, $2v_{su}$, increments in the extreme spacing $2b_m$ are in direct proportion to nonreversible increments $2\Delta c_s$ in the extreme spacing $2c_n$=2c.

A new fracture parameter Crack Volume Ratio (CVR) is the ratio V_g of the increment ΔM_g of the volume $M_g = A_g B_g$ enclosed by the surfaces of a growing crack at the moment of interest to the volume $M = A B$ of the same crack at the same moment but for the imaginary state of the PD without structural damage and internal stresses. Here A_g and A are in-plane areas of the ideal crack, B_g and B are the crack-tip thickness. When applied to the SST, the factors of thickness reduction $\beta_g = B_g/B$, $\beta_s = B_{ss}/B$ and $\beta_u = B_{su}/B$ are equal in magnitude. The V_g value consists of elastic

$$V_g^{el} = \left(1 + C_{mc}\frac{\sigma_g^{eff}}{E}\right)\left[1 + C_{nc}\frac{\sigma_g^{eff}}{E} + \frac{2\delta_g}{\pi\left(\rho_n c\right)^{0.5}}\right]\beta_g - 1 \qquad (1)$$

and plastic

$$V_g^{pl} = \frac{2h_g\beta_g}{\pi\left(\rho_n c\right)^{0.5}}\left(1 + C_{mc}\frac{\sigma_g^{eff}}{E}\right) \qquad (2)$$

components. Stress concentration factors C_{nc} and C_{mc} take the form $C_{nc} = F_{vc}\left[1 + 2\left(c/\rho_n\right)^{0.5} - k\right]$, $C_{mc} = F_{uc}\left[k + 2k\left(\rho_n/c\right)^{0.5} - 1\right]$, where $k = q/\sigma$ is the load biaxiality ratio, E is the Young's modulus. Compliances F_{vc} and F_{uc} are related to the points *"m"* and *"n"* on the actual crack profile, δ_g is the crack-tip opening displacement and h_g is the characteristic size of an Active Damage Zone (ADZ). The effective tensile stress σ_g^{eff} is taken as the sum of the internal stress σ_u and the applied stress σ. The level σ_u of fictitious loading is treated as a uniform tensile stress field that is internally generated during accumulation of structural damage represented in the analysis by the irreversible displacement v_{su}.

The SST is viewed as a process of continuous re-initiation with invariant values of the crack-tip driving forces h_g, r_g, and δ_g. The ADZ length, $r_g = l_g - c_g$ and its height $h_g = 2\left(b_g + v_g\right)\left[1 - \left(c_g/l_g\right)^2\right]^{0.5}$ are characterizing the generation of structural damage and δ_g governs crack extension within the Fracture Process Zone (FPZ). Crack extensions Δc_s are inversely proportional to the applied stress σ_s and values $\delta_{su} = 0$, h_{su}, δ_{ss}, h_{ss}, and r_{ss} are kept constant during crack growth. To link displacement v_{su} with the related value of stress σ_u, we use the following elastic solution $\sigma_u = E\, v_{su} / F_{vc}\left(2c_s + b_s\right)$ for the PD in question.

INSTABILITY AS A PRECURSOR OF STEADY-STATE TEARING

In practical terms, a focal issue is prediction of extreme load levels for a large-scale component from data collected on relatively small specimens. Such load levels are usually related to a single-point critical event *"c"* which separates slow (controllable) crack extension from fast (uncontrollable) one. In the UM analysis, instability is treated as a continuing transition from the final point *"p"* of the pseudo-steady blunting via the pseudo-steady tearing stage *"ps"* to the SST stage *"sa"* in Figure 2.

Point's *"p"* and *"s"* have the meaning of the lower and upper limits of the instability event *"c"*. The point *"p"* reflects some apparent state of the PD since it does not lie along the actual test record. However, the imaginary onset *"p"* of the pseudo-steady tearing is a distinct event derived directly from raw experimental data by using the diagram net-section stress $\sigma_N = \sigma c_f / \left(c_f - c\right)$ versus crack extension Δc [7]. Here c_f are the intersection points of the crack plane ($y = 0$) with the outer boundaries of the PD (see Figure 2), where $x = \pm\,(W\text{-}N)$. An appropriate example is the crack-

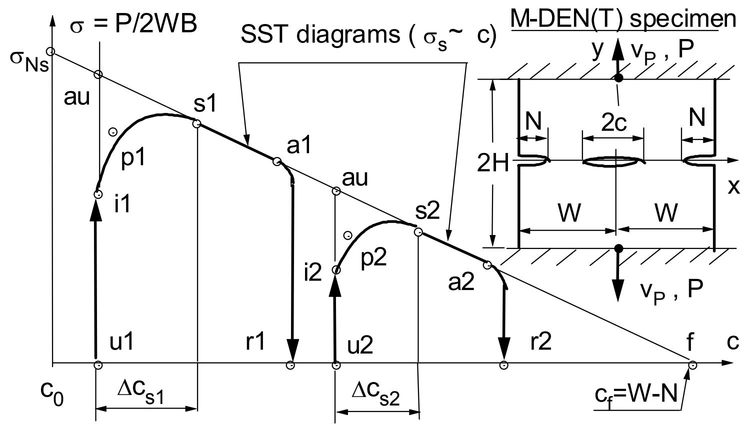

Figure 2: Scheme of test records, test events and SST diagrams for two Middle-Cracked Double-Edge-Notched Tension specimens.

extension data obtained in [8] which are presented here (Figure 3) in terms of the pseudo-steady diagrams. It can be seen that the critical points c1, c2 and c3 predicted with the R-curve concept are placed between the initial (p1, p2, p3) and the final (s1, s2, s3) points on tear diagrams.

The state *"c"* is difficult to define as the appearance of a distinct discontinuity in the mechanisms of ductile tearing. It is a continuous process giving an indication of equal fracture resistance either in advance of the point "*c*" or far after it proceeds. This is supported by a close agreement between the angles $T_{\sigma c} = (0.23 \pm 0.002)$ MPa/mm over wide ranges of crack growth initiated from different saw cuts (see Figure 3). Thus, it is practical to concentrate attention on a softening branch of the test records representing the highest load carrying capability of a center-cracked plate.

THE GLOBAL CONSTRAINT AND INSTABILITY PREDICTIONS

SST diagrams have variable characteristics depending on the interaction between the global in-plane constraint and the accumulation of structural damage within the fully-developed ADZ and FPZ. Displacements v_{su} and v_{st} and ADZ sizes h_{su} , h_{ss} , and r_{ss} serve as the easily obtainable damage parameters characterizing a transition from the stress-free state to the states "*u*" and "*s*". This transition is affected by changes in each constraint-related test parameter. Our attention is directed to SST diagrams for the

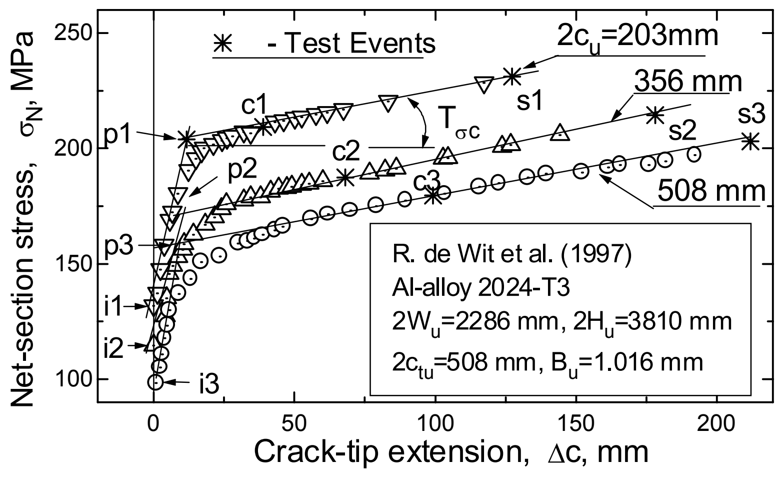

Figure.3. Test records (points) and related pseudo-steady diagrams (lines) for the M(T) specimens loaded to fracture under displacement control.

simplest PD usually referred to as the M(T) specimen. The latter is similar to the M-DEN(T) configuration in every way, with one exception, the depth N of both sharp notches (see Figure 2) is zero. One can ensure the conditions of almost zero straining along the crack plane by cutting the edge notches singly or together with a decrease in spacing $2H$ between the rigidly clamped boundaries. These variations in the PD geometry concentrate all the thinning, damage and cracking inside two localized necks spreading under the highest in-plane constraint to be expected.

The small specimens (see Figure 4) were made from 1.05-mm thick aluminium 1163AT having the composition similar to AL2024-T3 mentioned above. Its tensile properties: E = 73 GPa, 0,2% offset yield stress $\sigma_Y = 334$ MPa and ultimate strength $\sigma_{ult} = 446$ MPa are close to the characteristics E=71 GPa and $\sigma_Y = 345$ MPa presented in [8]. We intend to predict the instability events s1, s2 and s3 (Figure 3) for the largest flat panels that have ever been tested by the use of data presented in Figure 4. The M(T) specimens and the panels are close to geometrical similarity. An important point is that the global constraint is treated here as an elevation of the tensile stress σ_{Ns} averaged over the net-section of the PD. When normalized by the ultimate strength, this stress is denoted as a tear constraint factor, $\alpha_s = \sigma_{Ns} / \sigma_{ult}$. The values of α_s for the small and large M(T) specimens are, respectively, 0.834 and 0.485. It means that high-constraint data $(\alpha_s > \alpha_{sY})$ must be put into correspondence with low-constraint one $(\alpha_s < \alpha_{sY})$. Here $\alpha_{sY} = \sigma_Y / \sigma_{ult} = 0.749$ is the constraint factor corresponding to the lower limit of plastic collapse. For reference, the peak value of $\alpha_s = 1.112$ has been obtained in tests of the M-DEN(T) specimens with $2W$ = 240 mm, $2H$ =480 mm, N = 0.2 W, $c_u = 0.875 c_f$.

In our case of proportional scaling, a simplified (two-dimensional) version of the TL incorporates the parameters characterizing: (i) the panel geometry (B = 1.016 mm, $2W$ = 2286 mm, $2H$ = 3810 mm, $2c_s$ = 458, 712 and 932 mm); (ii) the boundary restraints (horizontal boundaries are rigidly clamped and vertical one are free-to-move); (iii) loading, loading history, and initial damage ($k = 0$, $\sigma_u = 0$, $v_u = 0$); (iiii) the material $(E = 71 GPa, \sigma_{ult} = 345 MPa)$ and finally the SST behaviour ($\rho_n = 0.262\, mm$, $F_{vc} \approx [\sec(\pi c_s / 2W)]^{0.5}$, $F_{uc} \approx -F_{vc}$, h_{su} = 3.948 mm, h_{ss} = 4.508 mm, and r_{ss} = 4.248 mm). Most of the SST parameters have been

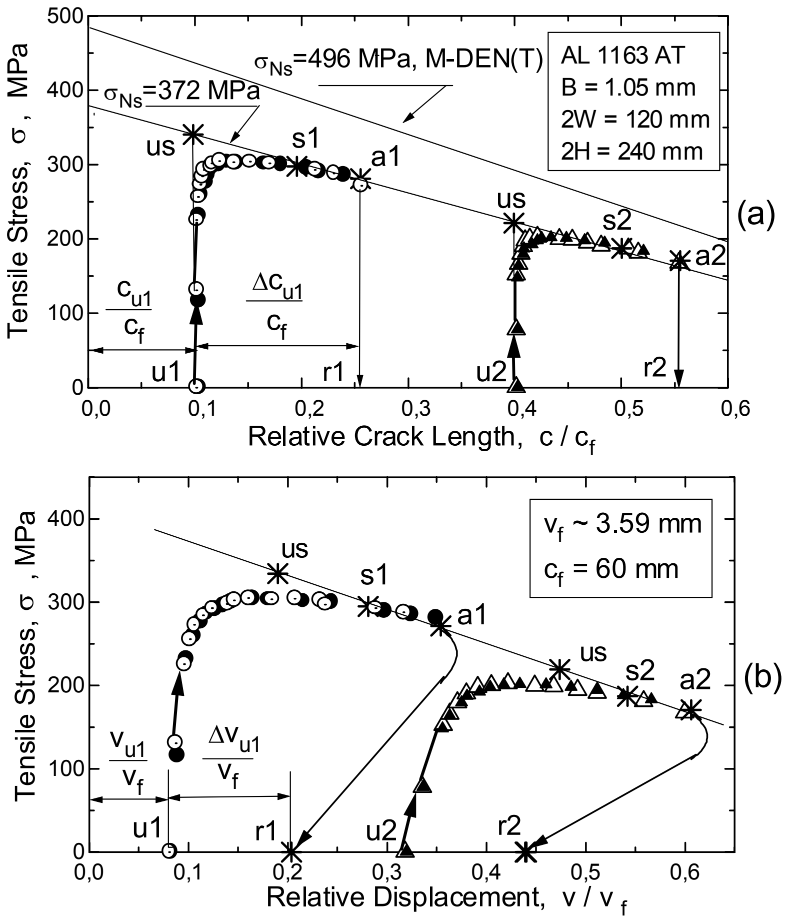

Figure 4: Basic test records, related SST diagrams and test events of practical importance for the M(T) specimens of small size.

derived from data presented in Figure 4 for the small M(T) specimens. Predicted and measured levels of the σ_s stress are as follows: 214.9 and 185 MPa for $2c_S$ = 458 mm, 171.5 and 148 MPa for $2c_S$ = 712 mm, 139.2 and 120 MPa for $2c_S$ = 932 mm. There is reason to think that the bias of theoretical and experimental data arise mainly from the influence of the loading systems in tests of the small and the large specimens. Machine compliance, coupled with specimen compliance, can have an effect on the crack driving force, *C*, on its derivative, *dC/dc*, [9], as well as on a transition from stable to unstable ductile crack growth. The ineffectiveness of the antibuckling guides used in [8] and mentioned in [3] is thought to be another main contributor of the above bias.

GENERAL REMARKS

The UM approach has the meaning of the simple mechanistic approximation based on the purely elastic single-parameter characterization of the overall response of crack borders to loading. It links together analyses of elasticity, plasticity, necking, damage and cracking and thereby offers an alternative to a popular concept "competition of fracture with plastic collapse" .

At the same time the UM is not an alternative to the conventional methodology of fracture mechanics as such. The well-defined sizes of ADZ and FPZ can be coupled with mechanism-based analyses of the crack-tip stress and strain employing a traction-separation law or void-containing cell elements..

ACKNOWLEDGEMENTS – Thanks are given to G.S.Volkov for very helpful cooperation and valuable discussions.

1. Naumenko, V.P., Kolednik, O., O'Dowd, N.P. and Volkov, G.S. (2000) In: *Life Assessment and Management for Structural Components.* **1**, pp.299-304, Troshchenko, V.T. (Ed.), Logos, Kiev.
2. Naumenko, V.P., Volkov, G.S. and Atkins, A.G (2001) In: *Proc. of 6th Intern. Conf on Biaxial/Multiaxial Fatigue and Fracture,* **2**, pp. 975-982, Freitas, M. (Ed.), Lisboa, Portugal.
3. Harris, C.E., Newman, J.C.,Jr., Piascik, R.S., and Starnes, J.H.,Jr. (1996). Änalytical Methodology for Predicting the Onset of Widespread Fatigue Damage in Fuselage Structure", *NASA TM 110293.* Hampton.
4. Lee, J.D., Liebowitz, H. and Lee, K.Y. (1996) *Engineering Fracture Mechanics* **55**, 61.
5. Naumenko, V.P. To be published in: *Mechanics of Solids in Russia and Ukraine,* Pisarenko, G.S. (Ed.). Znanie, Moscow.
6. Naumenko, V.P. (1998) In: *Fracture from Defects,* **2**, pp.1083-1088, Brown, M.M., de los Rios, E.R. and Miller, K.J. (Eds). Sheffield, UK.
7. Naumenko, V.P. (2000). In: *Life Assessment and Management for Structural Components.* **1**, pp.287-298, Troshchenko, V.T. (Ed.), Kiev.
8. de Wit, R., Fields, R.J., Low, S.R., Harne, D.E. and Foecke, T (1997). In: *Fatigue and Fracture Mechanics: ASTM STP 1296,* **27**, pp.451-468, Piasciak, R.S., Newman, J.C. and Dowling, N.E. (Eds), ASTM.
9. Kolednik, O. and Turner, C.E. (1994). *Fatigue Fract. Engng. Mater. Struct.,* **17,** 1129.